Theoretical study of the effect of nonlinear piezoelectricity on the pressure coefficient of the light emission in (111)-oriented InGaAs/GaAs quantum wells

S. P. Łepkowski
Unipress-Institute of High Pressure Physics, Polish Academy of Sciences, ulica Sokołowska 29, 01-142 Warszawa, Poland
(Received 22 November 2007; published 28 April 2008)

We investigate the effect of second-order piezoelectricity on the pressure coefficient of the light emission (dE_E/dP) in (111)-oriented InGaAs/GaAs quantum wells (QWs). In the framework of continuum theory of elasticity and piezoelectricity, we propose the analytic model of pressure tuning of the built-in electric field in a (111)-oriented zinc-blende QW, which takes into account the second-order (nonlinear) piezoelectric effect. Calculations performed using this model reveal that changes of the built-in electric field with pressure in (111)-oriented InGaAs/GaAs QWs are significantly enlarged by the effect of nonlinear piezoelectricity, in comparison to the case when linear piezoelectricity is used. Next, we discuss the influence of the effects of nonlinear piezoelectricity and nonlinear elasticity on dE_E/dP in (111)-oriented InGaAs/GaAs QWs as a function of In concentration and the QW width. We show that the effect of nonlinear piezoelectricity increases dE_E/dP in In-poor QWs and decreases dE_E/dP in In-rich QWs. The effect of nonlinear elasticity reduces dE_E/dP in the whole range of QW compositions. Contribution to dE_E/dP originating from the effect of nonlinear piezoelectricity depends more significantly on the QW width than the contribution coming from the effect of nonlinear elasticity.

DOI: 10.1103/PhysRevB.77.155327 PACS number(s): 77.65.Ly, 78.67.De

I. INTRODUCTION

Quantum confinement of free carriers in semiconductor nanostructures significantly alters the electronic and optical properties of these structures which makes them very attractive for numerous applications. Semiconductor nanostructures are in use today in a wide range of electronic and optoelectronic devices including high electron mobility transistors, light emitting diodes, and lasers. Description of electronic states in semiconductor nanostructures requires determination of intrinsic mechanical and electrical fields, which are present in these structures due to lattice misfit between constituents. Usually, the linear theory of elasticity and piezoelectricity is employed to calculate the strains and electrostatic potential, which are then linked to suitable band structure calculation methods to estimate the electronic states of a nanostructure.[1] In many cases, particularly when the lattice misfit between constituents is large, this simple approach turns out to be insufficient, and higher-order electromechanical effects should be taken into account.[1]

The nonlinear elastic and piezoelectric effects in semiconductors have attracted significant attention in the last few years. The effect of nonlinear elasticity, manifesting itself in dependence of elastic constants on hydrostatic pressure, has been primarily studied in InGaAs/GaAs strained structures. First, the effect of nonlinear elasticity was used to explain anomalously small values of the pressure coefficient of the band gap in InGaAs/GaAs compressively strained layers.[2,3] Second, it was found that the effect of nonlinear elasticity significantly reduces the built-in strain in InAs/GaAs quantum dots (QDs) and, therefore, it should be taken into account in accurate modeling of the strain in these nanostructures.[4] Third, it was shown that the effect of nonlinear elasticity is decisive in the determination of pressure coefficients of the light emission (dE_E/dP) in InAs/GaAs QDs.[5,6] Similar results were obtained for nitride heterostructures. In this case, the usage of the pressure dependence of elastic constants also caused reduction in dE_E/dP in wurtzite and zinc-blende InGaN/GaN and GaN/AlGaN quantum wells (QWs) and significantly changed the built-in strain in GaN/AlN QDs.[7,8] Recently, a study of the effect of nonlinear elasticity in tensile strained layers of nitride nanostructures has also been performed.[9]

The effect of nonlinear piezoelectricity in semiconductors was initially studied in the zinc-blende CdTe compound. It was found that in this material, the piezoelectric tensor significantly depends on hydrostatic strain.[10] Hydrostatic pressure photoluminescence experiments that were carried out on (111)-oriented CdTe-based QWs confirmed this result.[11] In the case of nitrides, the nonlinear piezoelectricity was initially investigated theoretically in wurtzite GaN and AlN compounds.[12] It was shown that the piezoelectric constants of these materials change with volume-conserving strain. Then, these results were used to explain the unusual dependence of the light emission on hydrostatic pressure in nitride QWs[13,14] and QDs.[15] Nonlinear dependences of the spontaneous and piezoelectric polarizations on biaxial strain in GaN, InN, and AlN compounds were also discovered.[16] Recently, the effect of nonlinear piezoelectricity has been studied in arsenides. Bester *et al.* have calculated the second-order piezoelectric coefficients for GaAs and InAs and have shown that the contribution of the second-order piezoelectric effect to the built-in electric field in (111)-oriented InGaAs/GaAs QWs and InAs/GaAs QDs is substantial.[17,18] They have also argued that experimental values of the piezoelectric coefficients for GaAs and InAs semiconductors are not actually the linear piezoelectric coefficients of these materials since they contain equally strong contributions originating from the first- and second-order piezoelectric effects.[17] Migliorato *et al.* have proposed to describe the effect of nonlinear piezoelectricity in InGaAs/GaAs heterostructures by using strain-dependent piezoelectric coeffi-

cients determined from the modified Harrison model of piezoelectric polarization.[19] The piezoelectric coefficients and the built-in electric fields in InGaAs/GaAs QWs obtained by using that model have exhibited good agreement with the experimental data. Finally, we would like to note that very recently, the second-order piezoelectric effect has been studied in InAs/InP and InAs/GaP QDs by using a semianalytic model of nonlinear piezoelectric polarization.[20]

In this paper, we present the study of the effect of nonlinear piezoelectricity on the pressure coefficient of the light emission (dE_E/dP) in (111)-oriented InGaAs/GaAs QWs. We show that, contrary to the linear piezoelectric effect, the second-order nonlinear piezoelectricity significantly changes the values of dE_E/dP in these structures. We compare the influence of nonlinear piezoelectricity on dE_E/dP with the contribution coming from the effect of nonlinear elasticity. The paper is organized as follows. In Sec. II, we derive the analytic model of pressure tuning of the built-electric field in (111)-oriented InGaAs/GaAs QWs, which takes into account the second-order piezoelectric effect. In Sec. III, we present the QW width and composition dependences of dE_E/dP for (111)-oriented InGaAs/GaAs QWs and discuss the contributions to dE_E/dP originating from the effects of nonlinear piezoelectricity and nonlinear elasticity. We draw our conclusions in Sec. IV.

II. NONLINEAR PIEZOELECTRIC EFFECT

In this paper, we consider a single InGaAs/GaAs QW grown on a GaAs substrate along the (111) crystallographic axis. We assume that (i) the structure is coherently grown, with no interfacial disorder, such that the continuum theory of elasticity and piezoelectricity can be applied; (ii) the thickness of the QW layer is much smaller than the thickness of the substrate, thus the in-plane lattice constant of the QW is entirely determined by the lattice constant of the substrate; (iii) interfaces are abrupt and the effect of indium segregation is excluded; and (iv) the structure is undoped, and the effect of free-carrier screening on the built-in electric field is negligible.

A. Pressure-dependent strains and stresses

To calculate the pressure tuning of strains in the QW layer and substrate, we use similar approach to that presented in Refs. 21 and 22. We designate the cubic axes by $x_1 \| [1,0,0]$, $x_2 \| [0,1,0]$, and $x_3 \| [0,0,1]$ and the QW axes by $x_1 \| [1/\sqrt{2}, -1/\sqrt{2}, 0]$, $x_2 \| [1/\sqrt{6}, 1/\sqrt{6}, -2/\sqrt{6}]$ (in-plane axes), and $x_3 \| [1/\sqrt{3}, 1/\sqrt{3}, 1/\sqrt{3}] \| [1,1,1]$ (direction of growth). The transformation matrix A that takes the cubic axes to the QW axes is then given by

$$A = \begin{pmatrix} 1/\sqrt{2} & -1/\sqrt{2} & 0 \\ 1/\sqrt{6} & 1/\sqrt{6} & -2/\sqrt{6} \\ 1/\sqrt{3} & 1/\sqrt{3} & 1/\sqrt{3} \end{pmatrix}. \tag{1}$$

Using the matrix A, one can express the elastic stiffness tensor of a zinc-blende crystal in the axes of the QW as follows:

$$C_{ij}^{111} = \begin{pmatrix} C_{11} - C/2 & C_{12} + C/6 & C_{12} + C/3 & C/3\sqrt{2} & 0 & 0 \\ C_{12} + C/6 & C_{11} - C/2 & C_{12} + C/3 & -C/3\sqrt{2} & 0 & 0 \\ C_{12} + C/3 & C_{12} + C/3 & C_{11} - 2C/3 & 0 & 0 & 0 \\ C/3\sqrt{2} & -C/3\sqrt{2} & 0 & C_{44} + C/3 & 0 & 0 \\ 0 & 0 & 0 & 0 & C_{44} + C/3 & C/3\sqrt{2} \\ 0 & 0 & 0 & 0 & C/3\sqrt{2} & C_{44} + C/6 \end{pmatrix}, \tag{2}$$

where C_{ij} are the elastic constants of a zinc-blende crystal in the cubic axes, and $C = C_{11} - C_{12} - 2C_{44}$.[21] For simplicity, we use the Voigt notation and indices i and j run from 1 to 6.

Now, let us focus on the strain-stress relation in the QW, which is subjected to external hydrostatic pressure. We use the generalized Hook's law in the axes of the QW as

$$C_{ij}^{111} \varepsilon_j^{111}(P) = \begin{cases} \sigma_i^{111}(P) - P, & i = 1-3, \\ \sigma_i^{111}(P), & i = 4-6, \end{cases} \tag{3}$$

where $\varepsilon_j^{111}(P)$ and $\sigma_i^{111}(P)$ are elements of the strain and stress tensors, respectively, expressed in the QW axes, and P is external hydrostatic pressure applied to the QW structure. We use the following boundary conditions:

$$\varepsilon_1^{111} = \varepsilon_2^{111} \equiv \varepsilon_\parallel = \frac{a_{sub}(P)}{a_{\mathrm{QW}}} - 1, \tag{4a}$$

$$\varepsilon_6^{111} = \sigma_3^{111} = \sigma_4^{111} = \sigma_5^{111} = 0, \tag{4b}$$

where a_{QW} is the bulk lattice constant of unstrained QW material and $a_{sub}(P)$ is the pressure-dependent lattice constant of the substrate.[21,22] Using Eqs. (2), (4a), and (4b), one can solve Eq. (3). We find

$$\varepsilon_3^{111} \equiv \varepsilon_\perp = -\frac{2(C_{11} + 2C_{12} - 2C_{44})\varepsilon_\parallel + 3P}{C_{11} + 2C_{12} + 4C_{44}}, \tag{5a}$$

$$\sigma_1^{111} = \sigma_2^{111} \equiv \sigma_\perp = \frac{6C_{44}[(C_{11}+2C_{12})\varepsilon_\parallel + P]}{C_{11}+2C_{12}+4C_{44}}, \quad (5b)$$

$$\varepsilon_4^{111} = \varepsilon_5^{111} = \sigma_6^{111} = 0. \quad (5c)$$

The above formulas are in agreement with the expressions previously derived for the pressure-dependent strains and stresses in a heterostructure oriented in an arbitrary crystallographic direction.[22] To complete the above model, we determine $a_{sub}(P)$. Since we consider the structures in which the thickness of the substrate is much larger than the QW width, the additional boundary condition for stresses, i.e., $\sigma_1^{111}=\sigma_2^{111}=0$, holds for the substrate. Then, solving Eq. (3) with this condition yields the well-known expression for $a_{sub}(P)$,

$$a_{sub}(P) = a_{sub,0}\left(1 - \frac{P}{C_{11,sub}+2C_{12,sub}}\right), \quad (6)$$

where $a_{sub,0}$ is the bulk lattice constant of an unstrained substrate and $C_{11,sub}$ and $C_{12,sub}$ are the elastic constants of a substrate material.[22]

B. Pressure-dependent electric field

The built-in electric fields in zinc-blende nanostructures originate from the piezoelectric effect, which manifests itself in the changes of the macroscopic polarization due to the strain. In a QW structure, the built-in electric field is perpendicular to the plane of the QW.[23] For a (111)-oriented QW, the electric field, which is expressed in the QW axes, is given by a vector field $E=[0,0,E_3^{111}]$. If the QW width is much smaller than the thickness of the substrate, the magnitude of E_3^{111} depends only on the component of the piezoelectric polarization normal-to-the-QW plane $P_{pz,3}^{111}$ and the static dielectric constant of the QW material χ,

$$E_3^{111} = -\frac{P_{pz,3}^{111}}{\chi\epsilon_0}, \quad (7)$$

where ϵ_0 is the vacuum permittivity. Equation (7) is also fulfilled when external pressure is applied to the QW structure, since in zinc-blende bulk materials the hydrostatic pressure cannot induce piezoelectric polarization and, therefore, the piezoelectric polarization of the substrate does not contribute to E_3^{111}. Now, we focus on the pressure dependence of $P_{pz,3}^{111}$.[22] It is convenient to first derive the formula for the piezoelectric polarization in the cubic axes P_{pz}^{001} and then to transform it to the QW axes to get $P_{pz,3}^{111}$. Let us then represent P_{pz}^{001} in the power series with respect to strain, retaining terms up to the second order in strain,

$$P_{pz,i}^{001} = \sum_j e_{ij}\varepsilon_j^{001} + \frac{1}{2}\sum_{jk} B_{ijk}\varepsilon_j^{001}\varepsilon_k^{001}, \quad (8)$$

where e_{ij} and B_{ijk} are the first-order and the second-order piezoelectric coefficients and ε_j^{001} are elements of the strain tensor expressed in the cubic axes. For crystals of zinc-blende symmetry, there are (i) 3 nonzero elements of the e_{ij} tensor, i.e., $e_{14}=e_{25}=e_{36}$, which can be expressed by one independent element e_{14} and (ii) 24 nonzero elements of the B_{ijk} tensor, which can be reduced to three independent elements, B_{114}, B_{124}, and B_{156}.[17] Thus, for the zinc-blende crystals, P_{pz}^{001} takes the specific form (see Ref. 24),

$$\begin{bmatrix} P_{pz,1}^{001} \\ P_{pz,2}^{001} \\ P_{pz,3}^{001} \end{bmatrix} = e_{14}\begin{bmatrix} \varepsilon_4^{001} \\ \varepsilon_5^{001} \\ \varepsilon_6^{001} \end{bmatrix} + B_{114}\begin{bmatrix} \varepsilon_1^{001}\varepsilon_4^{001} \\ \varepsilon_2^{001}\varepsilon_5^{001} \\ \varepsilon_3^{001}\varepsilon_6^{001} \end{bmatrix} + B_{124}\begin{bmatrix} (\varepsilon_2^{001}+\varepsilon_3^{001})\varepsilon_4^{001} \\ (\varepsilon_1^{001}+\varepsilon_3^{001})\varepsilon_5^{001} \\ (\varepsilon_1^{001}+\varepsilon_2^{001})\varepsilon_6^{001} \end{bmatrix} + B_{156}\begin{bmatrix} \varepsilon_5^{001}\varepsilon_6^{001} \\ \varepsilon_4^{001}\varepsilon_6^{001} \\ \varepsilon_4^{001}\varepsilon_5^{001} \end{bmatrix}. \quad (9)$$

In the particular case of a (111)-oriented QW, subjected to external hydrostatic pressure, one can obtain the tensor ε^{001} from the tensor ε^{111}, given by Eqs. (4a), (4b), and (5a)–(5c), using the transformation matrix expressed by Eq. (1). We find

$$\varepsilon_j^{001} = \begin{cases} \varepsilon_\alpha \equiv \dfrac{4C_{44}\varepsilon_\parallel - P}{C_{11}+2C_{12}+4C_{44}}, & j = 1-3, \\ \varepsilon_\beta \equiv -2\dfrac{(C_{11}+2C_{12})\varepsilon_\parallel + P}{C_{11}+2C_{12}+4C_{44}}, & j = 4-6. \end{cases} \quad (10)$$

Substituting Eq. (10) into Eq. (9) yields

$$P_{pz,1}^{001} = P_{pz,2}^{001} = P_{pz,3}^{001} \equiv e_{14}\varepsilon_\beta + (B_{114}+2B_{124})\varepsilon_\alpha\varepsilon_\beta + B_{156}(\varepsilon_\beta)^2. \quad (11)$$

Finally, by rotating P_{pz}^{001} to the QW axes and using Eq. (7), one obtains the formula for dependence of the built-in electric field in (111)-oriented QWs on hydrostatic pressure,

$$E_3^{111} = -\frac{\sqrt{3}}{\chi\epsilon_0}[e_{14}\varepsilon_\beta + (B_{114}+2B_{124})\varepsilon_\alpha\varepsilon_\beta + B_{156}(\varepsilon_\beta)^2]. \quad (12)$$

The first term represents the contribution coming from the linear piezoelectric effect. It agrees with a previously derived expression in Ref. 22. Note that, for $P=0$, the first term in Eq. (12) coincides with the results from Refs. 23 and 25. The other terms in Eq. (12) originate from the nonlinear (i.e., second-order) piezoelectric effect and have not been considered so far in analytic models of built-in electric fields in (111)-oriented QWs.

C. Results for InGaAs/GaAs quantum wells

Let us now discuss the results of calculations of the built-in electric field in (111)-oriented InGaAs/GaAs QWs obtained using the above model. The values of the material parameters for GaAs and InAs used in the calculations are listed in Table I. For InGaAs alloys, linear dependences of the parameters on In concentration are used. We have performed three series of calculations of E_3^{111}, taking into account (i) linear piezoelectricity with theoretical values of the coefficient e_{14} taken from Ref. 17 (of course, $B_{114}=B_{124}$

TABLE I. Parameters used for the calculation of the built-in electric field.

Parameter		GaAs	InAs
Lattice constant (Å)	a	5.6536[a]	6.0583[a]
Elastic constants (GPa)	C_{11}	118[a]	83[a]
	C_{12}	54[a]	45[a]
	C_{44}	60[a]	40[a]
Piezoelectric coefficients (C/m^2)	e_{14}	−0.23[b]	−0.115[b]
	B_{114}	−0.439[b]	−0.531[b]
	B_{124}	−3.765[b]	−4.076[b]
	B_{156}	−0.492[b]	−0.12[b]
	$e_{14,\mathrm{expt}}$	−0.16[b]	−0.045[b]
Dielectric constant	χ	12.5[c]	15.2[c]

[a]Reference 3.
[b]Reference 17.
[c]Reference 26.

$=B_{156}=0$ for the linear piezoelectricity); (ii) linear piezoelectricity with experimental values of the coefficient $e_{14,\mathrm{expt}}$ (see Table I); and (iii) second-order (nonlinear) piezoelectricity with the theoretical values of linear and quadratic piezoelectric coefficients.

In Fig. 1, we compare the values of E_3^{111} in InGaAs/GaAs QWs, at ambient pressure, obtained using our model with the results of atomistic calculations taken from Ref. 17. Since the results from Ref. 17 have the opposite signs to our results, we have changed their signs in Fig. 1 for comparative purposes. (Note that the sign of E_3^{111} depends on polarity of a QW structure.[23] The sign of our results is consistent with previous papers; see, for example, Refs. 23 and 27.) In Fig. 1, one can see that similarly to the results from Ref. 17, our model predicts that (i) the values of E_3^{111} calculated using

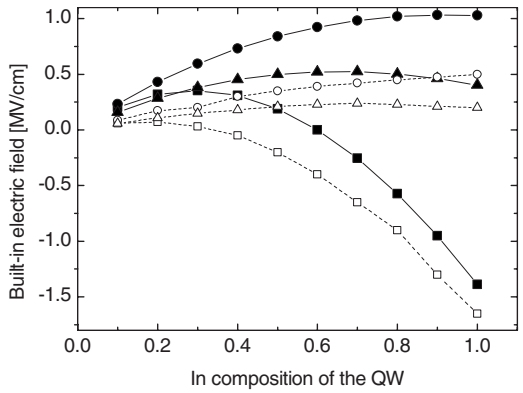

FIG. 1. The built-in electric field E_3^{111} in (111)-oriented InGaAs/GaAs QWs at ambient pressure, calculated using (i) linear piezoelectricity with theoretical values of the coefficient e_{14} (circles), (ii) linear piezoelectricity with experimental values of the coefficient e_{14} (triangles), and (iii) nonlinear piezoelectricity (squares), as a function of In concentration. The empty symbols correspond to the values of E_3^{111} reported in Ref. 17. Solid and dashed lines are added to guide the eyes.

nonlinear piezoelectricity reverse sign, going from positive numbers for In-poor QWs to a large negative field for In-rich QWs; and (ii) when linear piezoelectricity is used, the values of E_3^{111} are positive in the whole range of In concentrations. However, in Fig. 1, one can also observe a significant discrepancy between the values of E_3^{111} obtained using our model and the ones taken from Ref. 17. It is not possible, based only on the published data, to definitely point out the origin of this discrepancy. We would like to mention two differences in both approaches, which can lead to the observed discrepancy in the results. (i) One can suspect that the observed differences in E_3^{111} originate from differences in the strain fields obtained using our model and the atomistic approach presented in Ref. 17. Unfortunately, any values of the strain in the QWs are not reported in Ref. 17, so a direct comparison of the strains is not possible. One should also remember that in the atomistic approach, the strain field is inhomogeneous in the QW region.[17] Thus, in Ref. 17, the piezoelectric tensor is position dependent in the QW, which can also contribute to the discrepancy between the values of E_3^{111}, as observed in Fig. 1. (ii) In our model, we have assumed infinite barriers. This choice causes the electric field to be present in the QW region only and independent of the QW width. Note that the assumption of infinite barriers is very reasonable for the case of InGaAs/GaAs QWs, since the structures are usually grown on GaAs substrates and the total thickness of GaAs barriers (i.e., the thickness of the epitaxial barriers and the substrate) is much larger than the width of the QW. In the atomistic calculations, the widths of barriers are finite (usually of the order of tens of nanometers) and the electric field in the QW depends on the widths of barriers and the QW.[17]

In this place, we show that our model predicts the value of E_3^{111} in a very good agreement with experimental result for InGaAs/GaAs QWs, with In concentration of $x_{\mathrm{In}}=0.15$. According to Ref. 28, the value of E_3^{111} in 10 nm $In_{0.15}Ga_{0.85}As$/15 nm GaAs multi-QWs, which is deduced from absorption and electroreflectance spectra, is 190 kV/cm if In fluctuations are assumed to be present in the QW region or 165 kV/cm if In fluctuations are not taken into account. In order to compare our results with the experimental data, we should notice that the measurements in Ref. 28 were performed for multi-QWs. In the case of multi-QWs, the electric field in the QW region depends on the widths of wells and barriers and can be related to the value of E_3^{111} calculated for a single QW with infinite barriers by using the following formula:

$$E_{3,\mathrm{MQW}}^{111}=\frac{L_b\chi_{\mathrm{QW}}}{L_b\chi_{\mathrm{QW}}+L_{\mathrm{QW}}\chi_b}E_3^{111}, \tag{13a}$$

where χ_{QW}, χ_b, L_{QW}, and L_b are the static dielectric constants and the widths of QWs and barriers, respectively.[8,25] For the multi-QWs taken from Ref. 28, we obtain the value of $E_{3,\mathrm{MQW}}^{111}=166$ kV/cm when nonlinear piezoelectricity is considered, 204 kV/cm when linear piezoelectricity with theoretical values of the coefficient e_{14} is used, and 137 kV/cm when linear piezoelectricity with experimental values of the coefficient e_{14} is used. Interestingly, the value of $E_{3,\mathrm{MQW}}^{111}$,

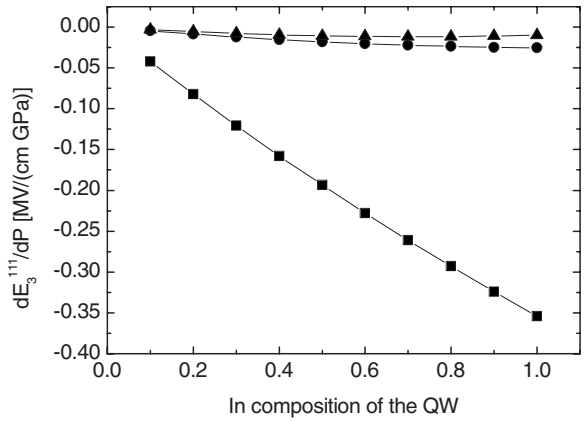

FIG. 2. The values of dE_3^{111}/dP in (111)-oriented InGaAs/GaAs QWs, calculated using (i) linear piezoelectricity with theoretical values of the coefficient e_{14} (circles), (ii) linear piezoelectricity with experimental values of the coefficient e_{14} (triangles), and (iii) nonlinear piezoelectricity (squares), as a function of In concentration. Solid lines are added to guide the eyes.

which is obtained using our model with the nonlinear piezoelectricity taken into account, is in very good agreement with the experimental result from Ref. 28, which was determined without assumption of composition fluctuations in the QWs.

Now, let us discuss the dependence of E_3^{111} on hydrostatic pressure for (111)-oriented InGaAs/GaAs QWs. In particular, we focus on a derivative of E_3^{111} with respect to P since this quantity is crucial for determination of the influence of the built-in electric field on the pressure coefficient of the light emission (dE_E/dP) in the considered QWs.[29] Using Eqs. (4a), (6), (10), and (12), one obtains the expression for dE_3^{111}/dP as follows:

$$\left.\frac{dE_3^{111}}{dP}\right|_{P=0} = \frac{2\sqrt{3}}{\chi\epsilon_0}\frac{\Delta}{D}\left\{e_{14} + \left(1 - \frac{a_{sub,0}}{a_{QW}}\right) \times \left[(B_{114} + 2B_{124})\left(\frac{1}{\Delta} - \frac{8C_{44}}{D}\right) + 4B_{156}\frac{C_{11} + 2C_{12}}{D}\right]\right\}, \tag{13b}$$

where

$$\Delta = 1 - \frac{a_{\mathrm{sub},0}(C_{11} + 2C_{12})}{a_{QW}(C_{11,sub} + 2C_{12,sub})}, \tag{13c}$$

$$D = C_{11} + 2C_{12} + 4C_{44}. \tag{13d}$$

In Fig. 2, we show the values of dE_3^{111}/dP for (111)-oriented InGaAs/GaAs QWs, which are calculated assuming linear piezoelectricity (circles and triangles) and nonlinear piezoelectricity (squares), as a function of In concentration. One can see that (i) the values of dE_3^{111}/dP are negative; (ii) the magnitudes of dE_3^{111}/dP increase with In concentration, and (iii) the magnitudes of dE_3^{111}/dP are significantly larger when the effect of nonlinear piezoelectricity is taken into account. From Figs. 1 and 2, one can determine whether the amplitude of the built-in electric field increases or decreases with an increase in hydrostatic pressure. Namely, when the linear theory of piezoelectricity is used, the values of E_3^{111} are positive (see Fig. 1) and the values of dE_3^{111}/dP are negative, thus the increase in hydrostatic pressure leads to the decrease in the magnitude of E_3^{111}. When nonlinear piezoelectricity is taken into account, the values of E_3^{111} are positive for In-poor QWs and negative for In-rich QWs. Since the values of dE_3^{111}/dP are negative in the whole range of In concentrations, it is clear that the increase in hydrostatic pressure causes a decrease (an increase) in the magnitude of E_3^{111} in In-poor (In-rich) QWs, when the effect of nonlinear piezoelectricity is considered. Pressure-induced changes of the magnitude of E_3^{111} influence the values of dE_E/dP due to the quantum confined Stark effect.[29] Namely, an increase (a decrease) in the magnitude of E_3^{111} with pressure results in a decrease (an increase) in the dE_E/dP.[29] Therefore, one can expect that the presence of the built-in electric field in (111)-oriented InGaAs/GaAs QWs results in (i) an increase in dE_E/dP, in the whole range of In concentrations, when the linear theory of piezoelectricity is used and (ii) an increase (a decrease) in dE_E/dP, for In-poor (In-rich) QWs, when nonlinear piezoelectricity is taken into account. Of course, the magnitude of changes of dE_E/dP, caused by the presence of the built-in electric field in the QWs, is expected to be larger when nonlinear piezoelectricity is used, since the magnitudes of dE_3^{111}/dP are larger in this case, in comparison to the case when linear piezoelectricity is taken into account.

III. PRESSURE COEFFICIENTS OF THE LIGHT EMISSION

In this section, we study dE_E/dP in (111)-oriented InGaAs/GaAs QWs. In particular, we investigate the influence of the effects of nonlinear piezoelectricity and nonlinear elasticity on the values of dE_E/dP in these structures. First, we describe the computational procedure and then we discuss the obtained results.

A. Computational details

In order to determine dE_E/dP, one has to compute the changes of the highest hole and the lowest electron states in the QW with respect to hydrostatic pressure. To reach this goal, we employ the effective mass theory developed for zinc-blende QWs grown along arbitrary crystallographic direction.[30] The effective mass Hamiltonians for electrons and holes include changes of the band edges caused by the strain and the built-in electric field in the system. Of course, for determination of pressure-induced changes in the strain and in the electric field, we use expressions derived in the previous section. To take into account the decrease in the QW width with pressure, we employ the following expression, which can be obtained from Eqs. (4a), (5a), and (6):

$$L_{\mathrm{QW}}(P) = L_{\mathrm{QW},0}\left\{1 + \frac{\left[2\frac{C_{11}+2C_{12}-2C_{44}}{C_{11,sub}+2C_{12,sub}}\left(\frac{a_{sub,0}}{a_{\mathrm{QW}}}\right) - 3\right]P}{3(C_{11}+2C_{12}) - 2(C_{11}+2C_{12}-2C_{44})\left(\frac{a_{sub,0}}{a_{\mathrm{QW}}}\right)}\right\}, \quad (14)$$

where $L_{\mathrm{QW},0}$ denotes the QW width at ambient pressure.

We focus only for direct interband transitions in (111)-oriented InGaAs/GaAs QWs, i.e., transitions from the conduction band minimum at the Γ point to the valence band maximum. Since in InGaAs/GaAs QWs, for P larger than 3 GPa, a crossover from direct to indirect emission is observed,[3,31] we compute the lowest band energies of electrons and holes for the values of P in the range between 0 and 3 GPa. Then, we determine the pressure dependences of the fundamental optical transition energy $E_E(P)$ for the QWs. When the linear theory of elasticity and piezoelectricity is used, $E_E(P)$ depends linearly on P and the pressure coefficient dE_E/dP is constant. The usage of nonlinear elasticity or nonlinear piezoelectricity results in a slight nonlinear dependence of E_E on P.[8,11] Note that in Ref. 11 the nonlinear dependence of $E_E(P)$ was experimentally discovered in CdTe QWs. The nonlinearity of $E_E(P)$ has not been detected so far in InGaAs/GaAs QWs, mainly due to the small value of the crossover pressure (3 GPa), at which the Γ and X levels of the conduction band cross.[31] In the calculations presented here, we obtain the nonlinear dependences $E_E(P)$, which cause the values of dE_E/dP to change with pressure. Therefore, we consider two pressure coefficients of the light emission: (i) the pressure coefficient in the vicinity of ambient pressure, $dE_E/dP|_{P=0}$, and (ii) the average pressure coefficient in the range of pressures from 0 to 3 GPa, $dE_E/dP|_{av}$. The values of $dE_E/dP|_{av}$ are estimated from a linear fit to $E_E(P)$. Note that the estimation of $dE_E/dP|_{av}$ is consistent with the experimental procedure of determination of dE_E/dP in InGaAs/GaAs QWs.[3,31]

In order to take into account the effect of nonlinear elasticity in determination of dE_E/dP in the InGaAs/GaAs QWs, we assume that the elastic constants of GaAs and InAs change with the total built-in hydrostatic pressure (P_{tot}) by

$$C_{ij}(P_{tot}) = C_{ij} + C'_{ij}P_{tot}, \quad (15)$$

where C'_{ij} are the pressure derivatives of the elastic constants and indices take the values $(ij)=(11),(12),(44)$, respectively. The values of P_{tot} are different in the barriers (and in the substrate) than in the QW, since the QW is compressively strained even at ambient pressure.[8] In the barriers, P_{tot} takes the same values as external hydrostatic pressure P. For the QW, P_{tot} is determined as

$$P_{tot} = -\tfrac{1}{3}\mathrm{Tr}(\sigma_{ij}) = P - \tfrac{2}{3}\sigma_{\perp}, \quad (16)$$

where $\sigma_{\perp}$ is the biaxial stress, which has been expressed by Eq. (5b).[8] In the calculations of dE_E/dP, we use the values of material parameters listed in Tables I and II. For InGaAs alloys, a linear dependency of the parameters on In concentration is used, except for the dependence of the energy gap which is calculated assuming a bowing parameter of −0.477.[33] In order to determine the confinement potentials for electrons and holes in InGaAs/GaAs QWs, we use the unstrained valence band offset of 0.052 eV, which was calculated for the InAs/GaAs system in Ref. 34.

B. Results and discussion

We present and discuss the results of calculations illustrating the influence of nonlinear piezoelectricity and nonlinear elasticity on dE_E/dP in (111)-oriented InGaAs/GaAs QWs.

1. In-poor InGaAs/GaAs quantum wells

Let us first discuss dE_E/dP in In-poor QWs. For concentrations of In lower than 0.4, the coherently grown InGaAs/GaAs QWs, with the QW width changing from a few nanometers to tens of nanometers, are experimentally accessible. In Fig. 3, we show the values of $dE_E/dP|_{av}$ (solid symbols) and $dE_E/dP|_{P=0}$ (empty symbols) calculated for 8 nm (111)-oriented InGaAs/GaAs QWs as a function of In concentration. We present the results obtained using (i) linear elasticity and linear piezoelectricity (circles and triangles), (ii) nonlinear piezoelectricity and linear elasticity (squares), (iii) linear piezoelectricity and nonlinear elasticity (pentagons), and (iv) nonlinear elasticity and nonlinear piezoelectricity (stars). One can see that, generally, the values of

TABLE II. Parameters used for the calculation of the pressure coefficient of the light emission.

Parameter		GaAs	InAs
Deformation potentials (eV)	a_c	−9.9[a]	−6.6[a]
	a_v	−1.2[a]	−1.0[a]
	d	−4.6[b]	−3.6[b]
Electron effective mass	m_e	0.067[c]	0.026[c]
Luttinger parameters	γ_1	6.98[c]	20.0[c]
	γ_3	2.93[c]	9.2[c]
Energy gap (eV)	E_g	1.519[c]	0.471[c]
Pressure derivatives of elastic constants	C'_{11}	3.9[b]	3.9[b]
	C'_{12}	4.8[b]	4.8[b]
	C'_{44}	0[b]	0[b]

[a]Reference 32.
[b]Reference 3.
[c]Reference 33.

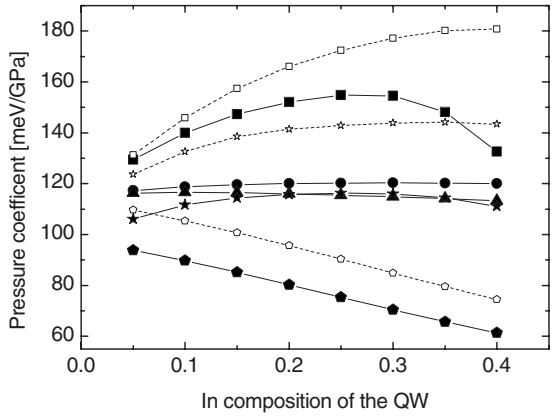

FIG. 3. The values of $dE_E/dP|_{av}$ (solid symbols) and $dE_E/dP|_{P=0}$ (empty symbols) calculated for 8 nm (111)-oriented InGaAs/GaAs QWs as a function of In concentration. Circles and triangles correspond to the results obtained using linear elasticity and linear piezoelectricity with theoretical and experimental values of the coefficient e_{14}, respectively. Squares, pentagons, and stars correspond to the results obtained using (i) nonlinear piezoelectricity and linear elasticity, (ii) linear piezoelectricity and nonlinear elasticity, and (iii) nonlinear elasticity and nonlinear piezoelectricity, respectively. Solid and dashed lines are added to guide the eyes.

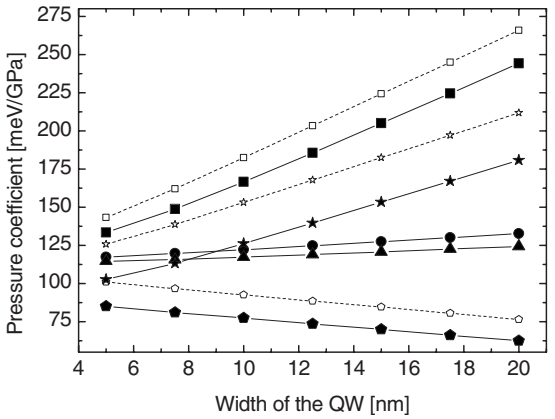

FIG. 4. The values of $dE_E/dP|_{av}$ (solid symbols) and $dE_E/dP|_{P=0}$ (empty symbols) calculated for (111)-oriented $In_{0.2}Ga_{0.8}As/GaAs$ QWs as a function of the QW width. Circles and triangles correspond to the results obtained using linear elasticity and linear piezoelectricity with theoretical and experimental values of the coefficient e_{14}, respectively. Squares, pentagons, and stars correspond to the results obtained using (i) nonlinear piezoelectricity and linear elasticity, (ii) linear piezoelectricity and nonlinear elasticity, and (iii) nonlinear elasticity and nonlinear piezoelectricity, respectively. Solid and dashed lines are added to guide the eyes.

$dE_E/dP|_{av}$ are smaller than the corresponding values of $dE_E/dP|_{P=0}$. The differences between $dE_E/dP|_{av}$ and $dE_E/dP|_{P=0}$ are larger for the case when the effect of nonlinear piezoelectricity (squares) is taken into account in comparison to the case when nonlinear elasticity (pentagons) is used. Let us now focus on the values of $dE_E/dP|_{av}$ obtained using nonlinear piezoelectricity (solid squares) and compare them with the values of dE_E/dP obtained using the linear theory of elasticity and piezoelectricity. One can see that the effect of nonlinear piezoelectricity increases dE_E/dP in In-poor InGaAs/GaAs QWs. This increase in dE_E/dP originates from a stronger decrease in the built-in electric field in the QW with pressure for the case when nonlinear piezoelectricity is taken into account, in comparison to the case when linear piezoelectricity is used. On the other hand, it is clear from Fig. 3 that the effect of nonlinear elasticity decreases the values of dE_E/dP in the InGaAs/GaAs QWs. This last finding is consistent with the previous results reported in Ref. 3. Interestingly, when both nonlinear effects, i.e., nonlinear elasticity and nonlinear piezoelectricity, are taken into account, the values of $dE_E/dP|_{av}$ (solid stars) are similar to the pressure coefficients obtained using the linear theory of elasticity and piezoelectricity.

In Fig. 4, we show the values of $dE_E/dP|_{av}$ (solid symbols) and $dE_E/dP|_{P=0}$ (empty symbols) calculated for $In_{0.2}Ga_{0.8}As/GaAs$ QWs as a function of the QW width. When linear elasticity and linear piezoelectricity are used (circles and triangles), dE_E/dP slowly increases with the QW width. The usage of nonlinear piezoelectricity (squares) leads to a strong linear increase in dE_E/dP with the QW width, which originates from significant pressure-induced decrease in the magnitude of E_3^{111}. When the effect of nonlinear elasticity (pentagons) is taken into account, the values of dE_E/dP slightly decrease with the QW width. Interestingly, for the QWs of small width, the contribution to dE_E/dP arising from the effect of nonlinear piezoelectricity is smaller than the contribution originating from the effect of nonlinear elasticity. For wide QWs, the influence of nonlinear piezoelectricity on dE_E/dP dominates over the effect of nonlinear elasticity.

2. In-rich InGaAs/GaAs quantum wells

Now, we discuss dE_E/dP in In-rich InGaAs/GaAs QWs. Let us first present the results obtained for (111)-oriented ultrathin InAs/GaAs QWs, and afterward we will demonstrate the dependence of dE_E/dP on In concentration in the InGaAs/GaAs QWs. [Note that high quality, ultrathin single InAs/GaAs QWs were successfully grown on (111)-oriented GaAs substrates.[35]] In Fig. 5, we show the values of $dE_E/dP|_{av}$ (solid symbols) and $dE_E/dP|_{P=0}$ (empty symbols) calculated for InAs/GaAs QWs as a function of the QW width. Again, the results have been obtained using (i) linear elasticity and linear piezoelectricity (circles and triangles), (ii) nonlinear piezoelectricity and linear elasticity (squares), (iii) linear piezoelectricity and nonlinear elasticity (pentagons), and (iv) nonlinear elasticity and nonlinear piezoelectricity (stars). One can see that in all the cases, dE_E/dP decreases with increasing QW width. It is also clear from Fig. 5 that the usage of nonlinear piezoelectricity reduces the values of dE_E/dP in InAs/GaAs QWs, which is in agreement with our previous qualitative considerations (see Sec. II C). As expected, the effect of nonlinear elasticity also results in the decrease in the dE_E/dP in the structures considered. The contribution to dE_E/dP originating from the effect of nonlinear elasticity is larger than the contribution coming from the effect of nonlinear piezoelectricity since the thickness of the QWs is small.

In Fig. 6, we show the values of $dE_E/dP|_{av}$ and $dE_E/dP|_{P=0}$ calculated for 1.5 nm InGaAs/GaAs QWs as a

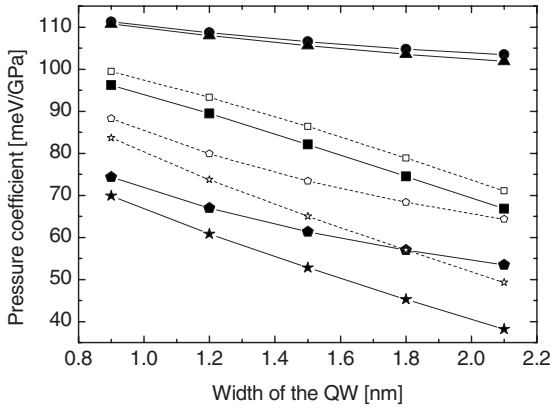

FIG. 5. The values of $dE_E/dP|_{av}$ (solid symbols) and $dE_E/dP|_{P=0}$ (empty symbols) calculated for (111)-oriented InAs/GaAs QWs as a function of the QW width. Circles and triangles correspond to the results obtained using linear elasticity and linear piezoelectricity with theoretical and experimental values of the coefficient e_{14}, respectively. Squares, pentagons, and stars correspond to the results obtained using (i) nonlinear piezoelectricity and linear elasticity, (ii) linear piezoelectricity and nonlinear elasticity, and (iii) nonlinear elasticity and nonlinear piezoelectricity, respectively. Solid and dashed lines are added to guide the eyes.

function of In concentration. One can see that (i) the effect of nonlinear piezoelectricity increases dE_E/dP in In-poor QWs and decreases dE_E/dP in In-rich QWs. This finding correlates with the pressure dependence of the magnitude of E_3^{111} previously discussed. (ii) The effect of nonlinear elasticity reduces the dE_E/dP in the whole range of In concentrations.

3. Comparison with experimental results

Finally, let us compare the calculated values of dE_E/dP with experimental results taken from the literature. There are

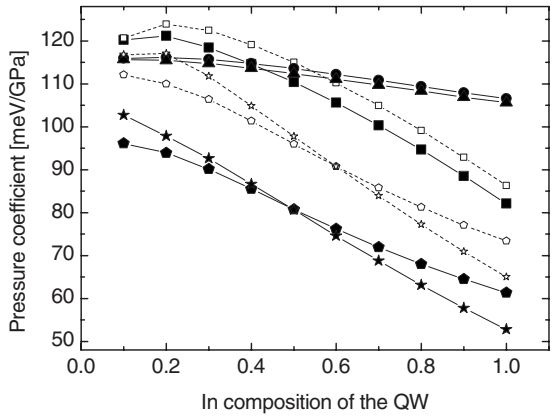

FIG. 6. The values of $dE_E/dP|_{av}$ (solid symbols) and $dE_E/dP|_{P=0}$ (empty symbols) calculated for 1.5 nm (111)-oriented InGaAs/GaAs QWs as a function of In concentration. Circles and triangles correspond to the results obtained using linear elasticity and linear piezoelectricity with theoretical and experimental values of the coefficient e_{14}, respectively. Squares, pentagons, and stars correspond to the results obtained using (i) nonlinear piezoelectricity and linear elasticity, (ii) linear piezoelectricity and nonlinear elasticity, and (iii) nonlinear elasticity and nonlinear piezoelectricity, respectively. Solid and dashed lines are added to guide the eyes.

only two experimental values of dE_E/dP which can be used to compare with our predictions. First, in Ref. 31, a pressure coefficient of $dE_E/dP=101$ meV/GPa was obtained for a single (111)-oriented $In_{0.23}Ga_{0.77}As/GaAs$ QW, with the well width of 2.4 nm. For the same structure, we obtain the following pressure coefficients: (i) 116 or 114.6 meV/GPa if linear elasticity and linear piezoelectricity are used, with theoretical or experimental values of the coefficient e_{14}, respectively (see Table I); (ii) 121.7 (127.7) meV/GPa if nonlinear piezoelectricity and linear elasticity are used; (iii) 89.4 (105.6) meV/GPa if linear piezoelectricity and nonlinear elasticity are used; and (iv) 95.1 (115.8) meV/GPa if nonlinear elasticity and nonlinear piezoelectricity are used. The numbers above correspond to the values of $dE_E/dP|_{av}$. In brackets, we have set the values of $dE_E/dP|_{P=0}$. Not surprisingly, the values of $dE_E/dP|_{av}$ are smaller than the values of $dE_E/dP|_{P=0}$. In the comparison between theoretical and experimental data, we focus on the values of $dE_E/dP|_{av}$ since they have been determined in a way that is consistent with the experimental procedure used in Ref. 31. Then, one can notice that the predictions based on linear elasticity and linear piezoelectricity are larger than the experimental result. The usage of nonlinear piezoelectricity increases $dE_E/dP|_{av}$ which enlarges the disagreement between experimental and theoretical results. However, the usage of nonlinear elasticity strongly reduces $dE_E/dP|_{av}$. In consequence, when both nonlinear effects are taken into account, the theoretical prediction is rather close to the experimental result.

Second, in Ref. 36, a pressure coefficient of $dE_E/dP=106.7$ meV/GPa was obtained for a structure of $In_{0.67}Ga_{0.33}As/GaAs$ five-QWs, with the well width of 10 nm. Unfortunately, the width of barriers was not reported for this structure. Therefore, we have performed calculations for a single 10 nm $In_{0.67}Ga_{0.33}As/Ga$ As QW. If linear elasticity and linear piezoelectricity are both used, we obtain $dE_E/dP=123$ or 110.1 meV/GPa for the theoretical or experimental values of the coefficient e_{14}, respectively. These predictions are in relatively good agreement with the experimental result. Surprisingly, the usage of nonlinear elasticity or nonlinear piezoelectricity leads to a significant discrepancy between theoretical and experimental values of dE_E/dP. Namely, when nonlinear elasticity is taken into account, we obtain $dE_E/dP|_{av}=43$ meV/GPa. The usage of nonlinear piezoelectricity results in an even stronger reduction in $dE_E/dP|_{av}$, which for this case is a negative number.

It is difficult to point out the origin of the discrepancy between our predictions and the experimental result reported in Ref. 36. One can speculate that the origin of the discrepancy comes from poor quality of the QWs used in high pressure experiment.[3] On the theoretical side, the atomistic calculations of the elastic and piezoelectric fields in (111)-oriented InGaAs/GaAs QWs under hydrostatic pressure are desirable. The usage of the Harrison model of nonlinear piezoelectricity, which is developed in Ref. 19, to study the coefficients dE_E/dP in these structures would also be valuable. However, it is not clear from Ref. 19 how the piezoelectric constant e_{14} would change in a material under biaxial and hydrostatic strains. Certainly, further experimental and theoretical studies of the dE_E/dP in (111)-oriented InGaAs/GaAs QWs are necessary. In this place, we would

like to add a comment on the experimental values of dE_E/dP for a series of In-poor (111)-oriented InGaAs/GaAs QWs, as reported in Ref. 3. Unfortunately, these results cannot be used for comparison with our predictions, since they were obtained using high excitation intensity photoluminescence measurements and the effect of the built-in electric field on dE_E/dP was severely reduced by the free-carrier screening.[3]

IV. CONCLUSIONS

In conclusion, we have studied the influence of the effect of second-order piezoelectricity on the coefficient dE_E/dP in (111)-oriented InGaAs/GaAs QWs. In the framework of continuum theory of elasticity and piezoelectricity, we have proposed the analytic model of pressure tuning of the built-in electric field in these structures, which takes into account the second-order (nonlinear) piezoelectric effect. Calculations performed using this model have revealed that changes of the built-in electric field with pressure, expressed by the magnitudes of dE_3^{111}/dP, are significantly enlarged by the effect of nonlinear piezoelectricity, in comparison to the case where linear piezoelectricity was used. Next, we have discussed the influence of the effects of nonlinear piezoelectricity and nonlinear elasticity on dE_E/dP in (111)-oriented InGaAs/GaAs QWs as a function of In concentration and the QW width. We have discovered that the effect of nonlinear piezoelectricity increases dE_E/dP in In-poor QWs and decreases dE_E/dP in In-rich QWs. The effect of nonlinear elasticity reduces dE_E/dP in the whole range of QW compositions. The contribution to dE_E/dP originating from the effect of nonlinear piezoelectricity depends more significantly on the QW width than the contribution coming from the effect of nonlinear elasticity.

ACKNOWLEDGMENTS

This work has been supported by the Polish State Committee for Scientific Research under Project No. 1P03B03729. Additionally, I would like to acknowledge the use of computing facilities at ICM UW. I also thank T. D. Young for careful proofreading of this paper.

[1] R. Maranganti and P. Sharma, *Handbook of Theoretical and Computational Nanotechnology*, edited by M. Reith and W. Schommers (American Scientific Publishers, Valencia, California, 2006), Chap. 118.
[2] M. D. Frogley, J. R. Downes, and D. J. Dunstan, Phys. Rev. B **62**, 13612 (2000).
[3] N. W. A. van Uden, J. R. Downes, and D. J. Dunstan, Phys. Rev. B **63**, 233304 (2001).
[4] S. W. Ellaway and D. A. Faux, J. Appl. Phys. **92**, 3027 (2002).
[5] B. S. Ma, X. D. Wang, F. H. Su, Z. L. Fang, K. Ding, Z. C. Niu, and G. H. Li, J. Appl. Phys. **95**, 933 (2004).
[6] J.-W. Luo, S.-S. Li, J.-B. Xia, and L.-W. Wang, Phys. Rev. B **71**, 245315 (2005).
[7] S. P. Łepkowski and J. A. Majewski, Solid State Commun. **131**, 763 (2004).
[8] S. P. Lepkowski, J. A. Majewski, and G. Jurczak, Phys. Rev. B **72**, 245201 (2005).
[9] S. P. Lepkowski, Phys. Rev. B **75**, 195303 (2007).
[10] A. Dal Corso, R. Resta, and S. Baroni, Phys. Rev. B **47**, 16252 (1993).
[11] R. Andre, J. Cibert, L. S. Dang, J. Zeman, and M. Zigone, Phys. Rev. B **53**, 6951 (1996).
[12] K. Shimada, T. Sota, K. Suzuki, and H. Okumura, Jpn. J. Appl. Phys., Part 2 **37**, L1421 (1998).
[13] G. Vaschenko, D. Patel, C. S. Menoni, N. F. Gardner, J. Sun, W. Gotz, C. N. Tome, and B. Clausen, Phys. Rev. B **64**, 241308(R) (2001).
[14] G. Vaschenko, D. Patel, C. S. Menoni, H. M. Ng, and A. Y. Cho, Appl. Phys. Lett. **80**, 4211 (2002).
[15] H. Teisseyre, T. Suski, S. P. Lepkowski, P. Perlin, G. Jurczak, P. Dluzewski, B. Daudin, and N. Grandjean, Appl. Phys. Lett. **89**, 051902 (2006).
[16] F. Bernardini and V. Fiorentini, Phys. Rev. B **64**, 085207 (2001).
[17] G. Bester, X. Wu, D. Vanderbilt, and A. Zunger, Phys. Rev. Lett. **96**, 187602 (2006).
[18] G. Bester, A. Zunger, X. Wu, and D. Vanderbilt, Phys. Rev. B **74**, 081305(R) (2006).
[19] M. A. Migliorato, D. Powell, A. G. Cullis, T. Hammerschmidt, and G. P. Srivastava, Phys. Rev. B **74**, 245332 (2006).
[20] J. Even, F. Dore, C. Cornet, L. Pedesseau, A. Schliwa, and D. Bimberg, Appl. Phys. Lett. **91**, 122112 (2007).
[21] E. Anastassakis, J. Appl. Phys. **68**, 4561 (1990).
[22] E. Anastassakis, Phys. Rev. B **46**, 13244 (1992).
[23] E. Anastassakis, Phys. Rev. B **46**, 4744 (1992).
[24] A. Schliwa, M. Winkelnkemper, and D. Bimberg, Phys. Rev. B **76**, 205324 (2007).
[25] D. L. Smith, Solid State Commun. **57**, 919 (1986).
[26] M. Grundmann, O. Stier, and D. Bimberg, Phys. Rev. B **52**, 11969 (1995).
[27] D. L. Smith and C. Mailhiot, J. Appl. Phys. **63**, 2717 (1988).
[28] P. Ballet, P. Disseix, J. Leymarie, A. Vasson, A.-M. Vasson, and R. Grey, Phys. Rev. B **59**, R5308 (1999).
[29] S. P. Lepkowski and J. A. Majewski, Phys. Rev. B **74**, 035336 (2006).
[30] R. H. Henderson and E. Towe, J. Appl. Phys. **79**, 2029 (1996).
[31] T. Sauncy, M. Holtz, O. Brafman, D. Fekete, and Y. Finkelstein, Phys. Rev. B **59**, 5056 (1999).
[32] S.-H. Wei and A. Zunger, Phys. Rev. B **60**, 5404 (1999).
[33] I. Vurgaftman, J. R. Mayer, and L. R. Ram-Mohan, J. Appl. Phys. **89**, 5815 (2001).
[34] K. Kim, G. L. W. Hart, and A. Zunger, Appl. Phys. Lett. **80**, 3105 (2002).
[35] M. Mashita, T. Numata, H. Nakazawa, Y. Kajikawa, B.-H. Koo, H. Makino, and T. Yao, Jpn. J. Appl. Phys., Part 2 **42**, L807 (2003).
[36] J. L. Sly and D. J. Dunstan, Phys. Rev. B **53**, 10116 (1996).